

Effect of the porous structure of graphite on atomic hydrogen diffusion and inventory

M.Warrier¹, R.Schneider², E. Salonen³, K. Nordlund⁴

¹ Institute for Plasma Research, BHAT, Gandhinagar, Gujarat, India - 382428

² Max-Planck-Institut für Plasmaphysik, D-17491 Greifswald, Germany

³ Laboratory of Physics, HIP, P.O.Box 1100, FIN-02015 HUT, Finland

⁴ Accelerator laboratory, P.O.Box 43, FIN-00014, University of Helsinki, Finland

E-mail: manoj@ipr.res.in

Abstract. A multi-scale model for particle diffusion in porous structures is used to study the effect of the porous internal structure of graphite on atomic hydrogen transport and inventory in graphite. The diffusion of trace amounts of atomic hydrogen are modeled as a trapping-detrapping mechanism within the porous network typical in graphites. Activation energies for the different traps are taken from experiments and from molecular dynamics simulations. It is seen that by varying the size of the voids between granules which constitute the graphite, the trace diffusion co-efficients of hydrogen vary by several orders of magnitude as reported in experiments ([1] and references therein) and it scales as L_{void}^2 , where L_{void} is the average size of voids in the graphite. Different diffusion mechanisms dominate at different graphite temperatures. Depending on the detrapping mechanism and on the internal structure of graphite, the jump lengths after each detrapping event can vary over a few orders of magnitude. This gives rise to the possibility of anomalous diffusion in graphite. The effect of closing the pores of graphite is also presented.

PACS numbers: 02.70.Ns, 02.70.Lq, 66.30.-h, 66.30.Ny

Submitted to: *Nuclear Fusion*

1. Introduction

Graphites and carbon fiber composites (CFCs) are used as plasma facing components and first wall materials in fusion devices. These have densities around 1.8 to 2.0 gms/cc as compared to the ideal density of crystallite graphite of 2.2 gms/cc. This indicates a void fraction of 5 – 10 % within these graphites. An illustration of the porous structure of isotopically compressed graphite, with typical length scales is shown in figure 1. It consists of granules of size around a few microns separated by voids which are typically of the order of 0.1 μ . The granules themselves are made up of crystallites (regions of crystal graphite) which are several nanometers wide. The crystallites are separated by micro-voids which are a few Å in size [2, 3, 4, 5]. Moreover there exists trap sites in the

graphite bulk with estimated concentrations of the order $10^{-3} - 10^{-5}$ per carbon atom [6, 7]. All this results in large, chemically reacting internal surfaces which the hydrogen can diffuse into, recombine on, or form hydrocarbons and get trapped in the bulk of the graphite.

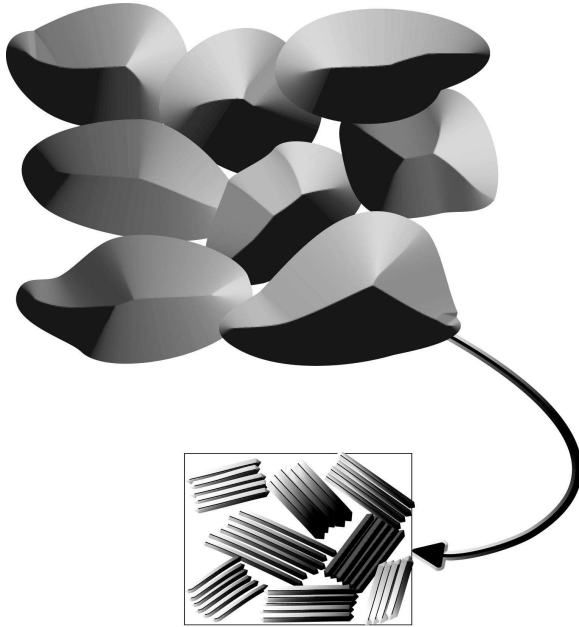


Figure 1. An illustration of the porous structure of graphite; The dark irregularly shaped objects stacked on top of each other represent micron sized granules separated by voids which are typically a fraction of a micron in size; The square section at the bottom of the figure is an illustration of the composition of a granule. It consists of 50-100 Å sized crystallites of graphite, separated by micro-voids of size 5-10 Å

Graphite surfaces exposed to fusion edge plasmas also get damaged by the incident energetic ions and neutrals from the plasma resulting in a high density of trap sites within the range of penetration of the incident ions ([3, 6] and references therein). In fusion reactors, energetic neutrons can penetrate deep into the graphite and create trap sites in the bulk. The incident hydrogen ions and neutrals which are not reflected at the surface are deposited in the graphite. There follows a wide range of possibilities for their transport and inventory as reviewed in [2, 3, 4, 8]. The deposited ions are neutralized at the graphite target and can either

- (i) get trapped in the region with a high density of traps, or in the bulk and
 - detrap as atoms or molecules and be solute within the internal surfaces,
 - undergo chemical reactions to form hydrocarbons or hydrogen molecules,
 or
- (ii) be solute within the internal surfaces and
 - be trapped at trap sites,
 - recombine to form molecules at the crystallite or granule surfaces,

In either case, the solute atoms and molecules diffuse along the voids and micro-voids with a probability of again being trapped, dissociated, or forming new molecules. There also exists finite probability of them re-entering the bulk granules or crystallites. Finally, when the hydrogen atom or molecule reaches the surface, it can be either thermally desorbed or knocked out by the incident ions.

Therefore, the relevant processes contributing to hydrogen transport are:

- (i) Trapping–detrapping,
- (ii) Recombination, dissociation and molecule formation,
- (iii) Desorption from graphite surface.
- (iv) Incident hydrogen deposition profile,
- (v) Damage profile,
- (vi) Trans–Granular–Diffusion,
- (vii) Diffusion along voids,

The above processes vary from the atomistic (i, ii and iii) to several nano-meters (iv, and v if we do not consider neutron damage) to tens of micro-meters (vi and vii). A multi-scale model has been developed to simulate these processes at the different scales [9, 10, 11] and to relate them to diffusion of hydrogen atom in porous graphite. This study applies to low concentration of H atoms and hydrogen molecules are not formed. However, this calculation gives an idea of possible transport preferences within the various regions, i.e. voids, granules and out of the surface (recycling). It also provides an insight into the trace hydrogen atom diffusion in porous graphite. An extension of the model to include hydrogen molecule formation and transport is under development.

The model for atomic hydrogen diffusion in graphite is described in the next section. Application of the model to graphites with different internal structures is presented in the third section. The results of these simulations are discussed in the fourth section. Finally the summary and outlook is presented. Though we do not model carbon fiber composites (CFCs) in this study, the models developed are directly applicable to CFCs.

2. Model for atomic hydrogen diffusion in graphite

Hydrogen atom diffusion in porous graphite is modeled as a random walk in a 3D porous structure with a variety of competing trapping-detrapping processes using a combination of kinetic Monte Carlo (KMC) [12, 13] and Monte Carlo diffusion (MCD) [14].

2.1. Creating the 3D porous geometry of graphite

An algorithm to generate a 3-D rectilinear parallelepiped with a specified void fraction and sub-structures having random shapes separated by voids/microvoids, based on the

algorithm presented by Graziani [15] for creating mixtures of alloys, was developed. It allows for the average size of the sub-structures, their smoothness and orientation to be specified. This facilitates creation of granules separated by voids or randomly oriented crystallites separated by micro-voids.

For a given volume, a statistical distribution is used to specify the width of a sub-structure that has a random shape. The sub-structures are created by populating basic blocks called cells which fill up the whole volume. The smoothness of the sub-structure depends on the cell-size. If the sub-structures are crystallites, random orientations are also specified. After each populating event wherein cells constituting a sub-structure are filled, the remaining void fraction, which is the fraction of empty cells, is checked. The process is repeated till the required void fraction is obtained. We choose a Poisson distribution for assigning the widths of sub-structures due to lack of data. figure.2 shows a typical porous graphite structure generated by the above described algorithm.

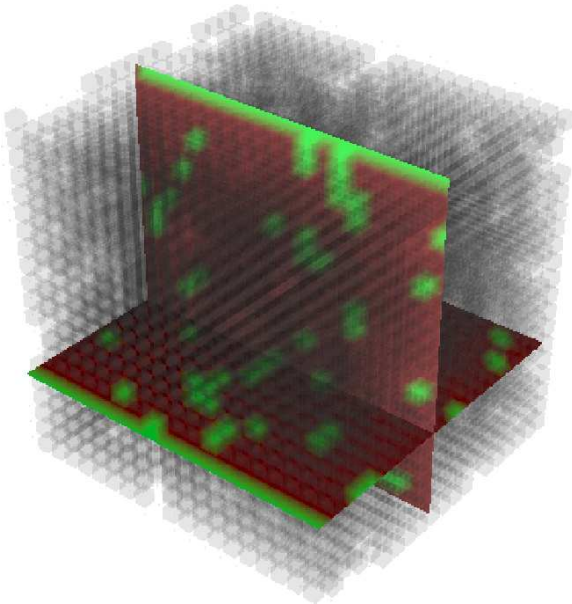


Figure 2. A typical porous graphite structure generated by statistically populating cells. Occupied cells are assigned a value 1 and unoccupied cells are assigned a value 0. The occupied cells are made partially transparent so that the internal structure is also seen. Two opaque planes are drawn perpendicular to each other so as to distinguish the occupied cells from the unoccupied cells at their location.

2.2. The diffusion model

Diffusion is considered to be a thermally activated process whose coefficients are usually presented [1, 7] in the form

$$D = D_o e^{\frac{-E_m}{k_B T}} \quad (1)$$

with units of $length^2/time$, D is the diffusion coefficient and D_o is the the pre-factor of the diffusion coefficient. E_m is the activation energy of the detrapping process and T is the temperature. In the trapping-detrapping limited diffusion regime, this can be interpreted as

$$D = \omega_o L^2 e^{\frac{-E_m}{k_B T}}. \quad (2)$$

The physical meaning of D_o is obvious from Eqn.1 and Eqn.2. It is the product of the number of attempts ω_o to detrapp from a potential well of depth E_m per second, and the square of the average length jumped, L^2 , after a detrapping event. The second part of Eqn.1 is the probability of detrapping.

2.2.1. Modeling diffusion using Kinetic Monte-Carlo ω_o , E_m and L are inputs to the Kinetic Monte-Carlo method, which initializes particles and simulates a random walk of the particles in the porous geometry with the choice of particle being weighted by the BKL Algorithm [13]. The time increment for each jump event is given by [12], representing the time interval between two events sampled from a sum of Poisson processes:

$$\Delta t = -\frac{\log U}{N \sum_i \omega_i} \quad (3)$$

where U is a uniform random number between 0 and 1 and i are the various kinds of detrapping events possible (eg: desorption, detrapping). At the end of such a simulation the mean square deviation of the N hydrogen atoms per unit time yields the diffusion co-efficient of hydrogen. Such a study has been done to find out the trans-granular-diffusion coefficient (D_{TGD}) of hydrogen [10] where we scaled up from nanometers to microns.

Note that in Eqn.3, N and ω_i are both in the denominator. This indicates that Δt becomes small when the number of atoms simulated is large or when the temperature simulated is high. This, along with the fact that only one particle moves per time step is a serious limiting factor for using KMC at the macro-scales, since it constrains the total time simulated. The advantage of using KMC is that it yields the diffusion co-efficient which can then be used as an input to other algorithms which do not have the limitations of the KMC method.

2.2.2. Modeling diffusion using Monte-Carlo Diffusion Given a diffusion co-efficient D , the Monte-Carlo diffusion (MCD) method is a quick and handy way to implement diffusion in an arbitrary geometry. The diffusion can be represented as a random walk of the N particles with the jump size given by

$$\Delta r = \sqrt{2 D \Delta t} \zeta \quad (4)$$

where Δt is the time step and ζ is sampled from a random number distribution satisfying $\langle \zeta \rangle = 0$ and $\langle \zeta^2 \rangle = 1$. This representation is valid for $\frac{D}{\nabla D} \gg \sqrt{2 D \Delta t}$. Interactions can be easily included in the simulation by increasing or decreasing (depending on whether the interactions are sources or sinks) the number of particles diffusing at each time step by $e^{-\frac{\Delta t}{\tau}}$ where τ is the characteristic time for the interaction to occur. Eqn.4 is derived using the differential calculus of stochastic processes called *Itô calculus* [14].

2.2.3. Bulk diffusion algorithm The algorithm for hydrogen transport is shown in figure 3. The atoms at the void–granule interface and within the voids are transported using KMC, which also provides the time step Δt for the simulation. Particles reaching the surface have a probability of being desorbed. This is also handled within the KMC algorithm. A Monte Carlo diffusion algorithm [14] is implemented for treating the trans–granular–diffusion (TGD). The diffusion coefficient for TGD, D_{TGD} , obtained

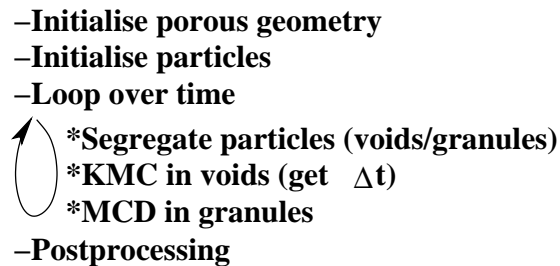


Figure 3. The Bulk simulation model algorithm

from the simulations of TGD at the meso–scales is used as input to the MCD algorithm. This is an example of how results from microscopic studies at the smaller scales is used to model transport at the larger scales.

As the hydrogen atoms diffuse along the void surfaces, if they come closer than a specified minimum distance to each other, they recombine to form a hydrogen molecule (Smoluchowski boundary condition [16]). Similarly, if the atoms come closer than a given distance to a trap, they are trapped. These minimum distances can be calculated from atomistic simulations or experiments. Dissociation and transport of hydrogen molecules within voids and on void–granule surfaces are included in the KMC algorithm. Recombination, dissociation, etc., in the granule bulk can also be easily included within a MCD algorithm. Therefore hydrogen transport, recombination, dissociation and desorption can all be studied in a porous 3D geometry within the above model. In this study we limit ourselves to studying the trace hydrogen diffusion in porous graphite.

3. Simulation of hydrogen atom transport in different graphites

Transport of atomic hydrogen in porous graphite with open and closed pores have been studied at different temperatures of graphite.

3.1. Description of the geometry

A cubic granular structure of length $5 \times 10^{-5}m$ is created (figure 4). Using the algorithm described in Section.2.1, a typical bulk graphite structure consisting of granules and voids is generated. This typically accommodates 8000 granules using a *element-length* of $2.5 \times 10^{-6}m$. The *cell-length* chosen is $5 \times 10^{-7}m$. These values for *element-length* and *cell-length* correspond to realistic granule and microvoid sizes. Periodic boundary conditions are applied along the **X** and **Y** directions, which are the directions parallel to the graphite surface. Along the **Z** direction, which lies perpendicular to the graphite surface, the structure is replicated for $Z > 0$. The graphite surface lies at $Z = 0$ and faces the plasma located in the negative **Z** direction.

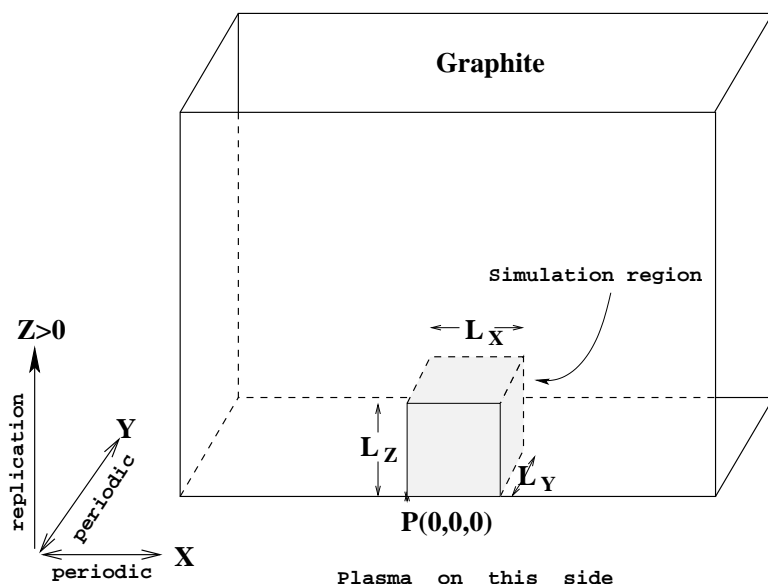


Figure 4. The Bulk simulation model geometry. Note the axes and boundary conditions specified at the bottom left hand corner of the figure.

3.2. Initializing the hydrogen atoms

The incident hydrogen deposition profile and the damage profile can be obtained from TRIM/TRIDYN [17, 18] simulations which simulate the momentum transfer processes in an isotropic solid. At the end of such a simulation the incident atoms lose their energy and thermalize with the target. Our simulations start from the point where these simulations end. 1000 thermalized H atoms are uniformly distributed in the X-Y plane. The atoms have a Gaussian distribution along the Z axis, centered at a depth of 600 Å from the surface with a width 10 Å. The void fraction was chosen to be 0.1 and therefore most of the particles end up inside granules. The rest of the particles are assumed to be solute H on the void-granule interface.

Damage creation and trapping at damage sites by incident ions/atoms is modeled by distributing the incident hydrogen atoms using a Gaussian depth distribution. This is a valid assumption since the damage due to incident hydrogen ions/atoms is restricted to a few nanometers at most, while we simulate the hydrogen atom transport over several tens of microns. The exact range and the exact damage or deposition profile does not influence the transport properties which we address in this study.

3.3. Other inputs

The inputs to the code are from a mixture of experimental results and MD simulations. The activation energy for trapping–detrapping within the granule is taken to be 2.7 eV since the TGD diffusion coefficient obtained from our simulations using this value lies nicely in the middle of the range reported in experiments [1]. Within the KMC algorithm, the activation energy for desorption is taken to be 1.91 eV [19]. The activation energy for surface diffusion is taken to be 0.9 eV, with a jump attempt frequency of 10^{13} s^{-1} and a jump step length of 34.64 \AA to match the surface diffusion coefficient reported in [7]. Activation energy for getting into the granule for a solute H atom on a granule surface is assumed to be same as the activation energy for TGD. The simulations are carried out at target temperatures between 300 K and 1500 K in intervals of 300 K. The particles were followed for 10^6 steps.

4. Results for trace hydrogen atom transport

Based on our inputs, approximately 10 % of the H atoms must be initialized on the void-granule surfaces and the rest inside the granule bulk. Results of the simulation are presented in three subsections as follows:

- Cross regional transport as a function of graphite temperature. The different regions are the internal void-granule surfaces, the granule itself and the bulk graphite surface.
- The trace diffusion coefficient of hydrogen in porous graphite.
- Effect of closed pores on the hydrogen transport.

4.1. Cross regional transport of hydrogen atoms in porous graphite

Initial results from our simulations were presented in [11] and are reproduced as figure 5. The final number of particles in different regions are plotted as a function of target temperature (figure 5). In this plot N stands for the number of particles in a region, and the region is given as a subscript. A plot of the hydrogen atom positions in the \mathbf{Z} direction at the end of the simulation within the 3D porous structure is shown in figure 6 for 300 K, 900 K and 1500 K with the time taken for 10^6 KMC steps being $1.38 \times 10^6 \text{ s}$, $1.15 \times 10^{-4} \text{ s}$, and $9.25 \times 10^{-7} \text{ s}$ respectively. Analysis of these two results

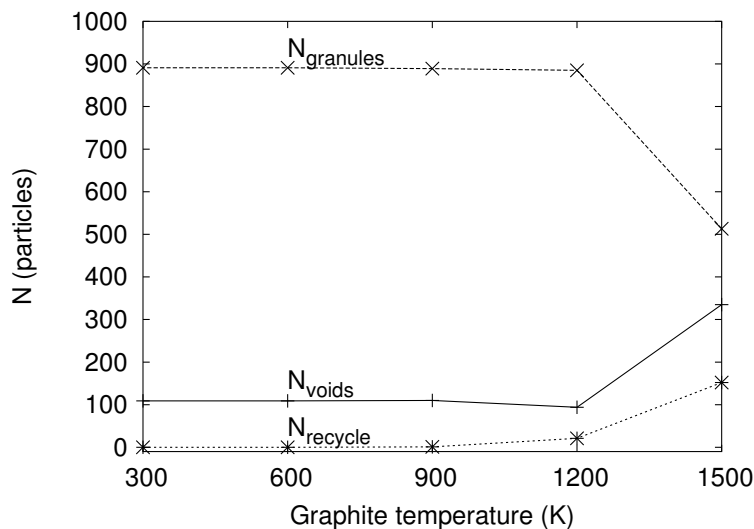


Figure 5. Number of particles in different regions at the end of a million KMC steps

show that:

- At temperatures < 900 K the atoms in the different regions do not cross over. Most of the transport is due to surface diffusion of atoms on the void-granule surface due to the low migration energy for surface diffusion ($\sim 0.9eV$). At these low temperatures, the hydrogen atoms which are assumed to be thermalized with the graphite, do not have enough energy to either get into a granule ($\sim 2.5 - 4.0eV$) or to desorb ($\sim 1.9eV$). The atoms in the granules have a much smaller diffusion coefficient due to their high migration energy ($\sim 2.5 - 4.0eV$) and due to the small microvoid sizes.
- At graphite temperatures ≥ 900 K the atoms start migrating across the different regions. This is seen in figure 5 where the number of particles in different regions show variation only above 900 K. It is also seen in figure 6-(iii), where the atoms in the granule (filled circles) show visible diffusion broadening indicating that diffusion in the granule is also taking place.
- Desorption of hydrogen atoms from the surface (denoted by N_{recycle} in figure 5) starts off somewhere between 900 K and 1200 K. Such behavior for hydrogen atom desorption is observed in experiments [7, 20].
- Surface diffusion allows atoms to penetrate to several microns in the porous graphite (figure 6. Note that 10^6 time steps correspond to different times of simulation at different graphite temperatures since the time step is determined by the KMC algorithm (see Eqn.3). The typical time taken for hydrogen atoms to penetrate several Å into the graphite is ~ 15 days at 300 K, less than a millisecond at 900 K and around a microsecond at 1500 K.

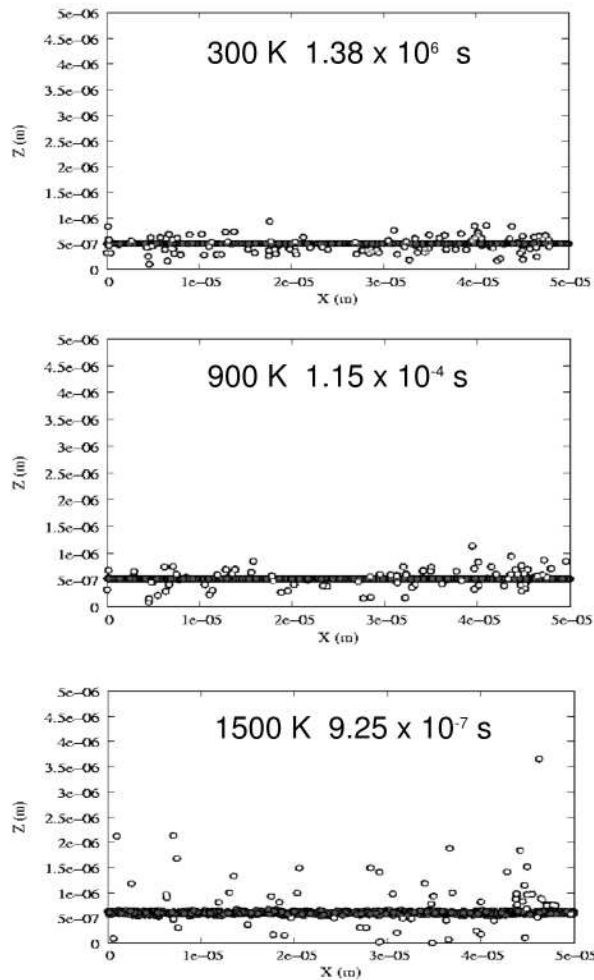


Figure 6. Atomic diffusion range. The filled circles indicate atoms in granules and empty circles indicate atoms in voids. The temperature of graphite and the time simulated is shown in the brackets above the figure. The surface lies at $Z = 0$

4.2. Trace diffusion coefficient of hydrogen atom in porous graphite

The trace diffusion coefficient of the hydrogen atoms, obtained by finding out the average mean square deviation per unit time of the N particles in the simulation, is plotted on a log-scale as a function of $1000/T$ K^{-1} in figure 7 (labeled **DiG**). We see that the diffusion coefficients are much larger than the reported values for bulk diffusion in graphite [1]. This is because surface diffusion dominates in the simulation at temperatures less than 1000 K. We also see that there exists two different channels for diffusion by the two different slopes that are seen in figure 7. The higher slope at temperatures greater than 1000 K indicates a higher migration energy for the diffusion and is due to adsorption-desorption (E_m for this process being 1.9 eV). It dominates the diffusion at higher temperatures due to its larger jump size. Surface diffusion was constrained to jumps on the surface whereas particle desorption from a surface allows the particle to

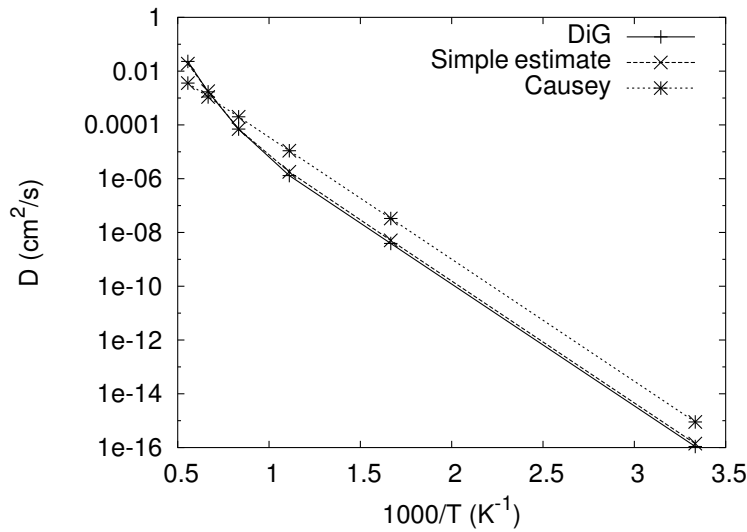


Figure 7. Diffusion coefficient for hydrogen in porous graphite compared with a simple estimate similar to the two kinds of jumps model presented in [11] and Causey's result for surface diffusion in graphite [7], wherein a surface diffusion coefficient varying as $1.2 e^{\frac{-0.9}{k_B T}}$ is proposed from experimental observations

jump across voids.

We also plot an analytical estimate of the diffusion coefficient. Here we consider two kinds of jumps, one for surface diffusion and the other for adsorption-desorption. The model is similar to that presented in [11] for jump parameters corresponding to surface diffusion and adsorption-desorption in voids. Specifically, we use Eqn.5,

$$D_{TwoJmp} = \frac{N}{6} \left(\frac{\omega^{SD}(L^{SD})^2 + \omega^D(L^D)^2}{\sum_{i=1}^N (-\ln(U_i))} \right) \quad (5)$$

where D_{TwoJmp} is the diffusion coefficient of a particle which is allowed to do a random walk consisting of N steps in the voids within graphite by means of surface diffusion (represented by terms with a superscript SD) and an adsorption-desorption (represented by terms with a superscript D) mechanism. ω is the number of surface diffusion / desorption jumps per second and is given by

$$\omega^{SD,D} = \omega_o^{SD,D} e^{\frac{E_m^{SD,D}}{k_B T}} \quad (6)$$

where ω_o is the jump attempt frequency which is assumed to be a phonon driven activation process and is of the order of the phonon frequency of graphite ($\sim 10^{13} \text{sec}^{-1}$). E_m is the migration energy. The $-\ln(U_i)$ term in the denominator comes from sampling a Poisson distribution for obtaining the time interval between any two successive jumps as given in Eqn. 3.

The reported values for diffusion coefficient for surface diffusion ($1.2 e^{\frac{-0.9}{k_B T}}$) from experimental observations [7] is also plotted in figure 7. This expression does not have

a adsorption-desorption contribution to diffusion and therefore shows only one slope. There is a difference of almost an order of magnitude in the values of the surface diffusion coefficient obtained from our simulation and [7]. This is inspite of the choice of step size of surface diffusion being based on [7]. The reasons for the mismatch are:

- We are constrained in our simulation by the available RAM and can create granules of average size 2.5 microns as opposed to the 10 micron average granule sizes of the graphite used in [7].
- The diffusion is occurring in a complex geometry, and evaluating the diffusion coefficient, ($D = \lim_{t \rightarrow \infty} \frac{1}{2dt} [r(t) - r(o)]^2$), assuming a dimensionality (d) of 3 is naive. Special techniques must be used to evaluate the diffusion coefficients in a porous disordered geometry [21].

We then carry out simulations by switching off the surface diffusion and the adsorption-desorption mechanisms, keeping only the trapping-detraping mechanism with 4.3 eV trap energies. The simulation was on a highly resolved structure using a cell size $1 \times 10^{-8}m$ which required around 1/2 GB of RAM. The RAM requirement scales as $(L/CellSize)^3$ since the geometry details have to be stored for quick access in the RAM, where L is the length of one side of the simulation volume and $CellSize$ is the size of a cell. Note that L must be large enough to at least contain a few granules (of size $\sim 1micron$) to realistically simulate bulk diffusion. We choose L to be 5 microns so that there exists around 125 granules in the 3D simulation volume. The simulations were carried out at 1200 K, 1500 K and 1800 K to compare with the results for bulk diffusion by Causey et. al. reported in [1]. The results of these simulations are presented in figure 8. The diffusion coefficient obtained lies in the range of reported experimental

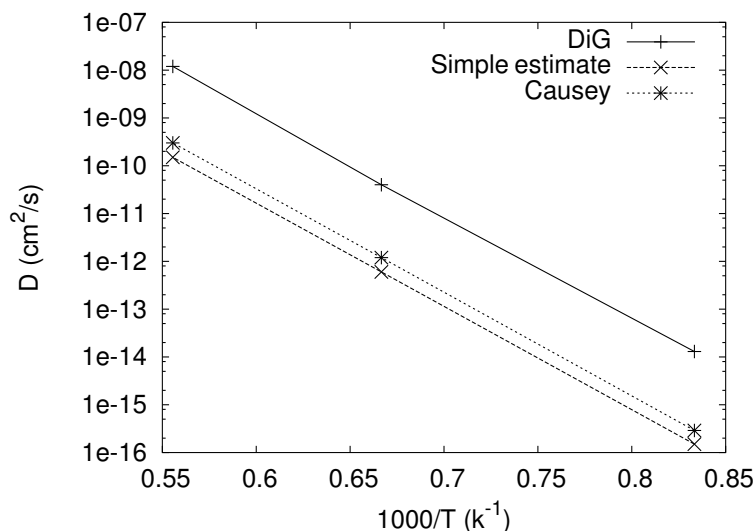


Figure 8. Diffusion coefficient for hydrogen in porous graphite with surface diffusion and adsorption-desorption mechanisms on void surfaces switched off. This is compared with with a simple estimate based on a 3-D random walk and Causey’s result for bulk diffusion in graphite [7]

results for bulk diffusion in graphite. It differs by almost two orders of magnitude as compared with the results by Causey et. al. The main reason is the granule size (and therefore the void size) we choose is $1/10^{th}$ the value reported in Causey's experiment due to RAM limitations in our simulation. Simulation of a realistic bulk structure will require around 500 GB of RAM. However, using the results of this simulation in a simple estimate including a modified void size which is typically 10 times greater than in the simulation, we are able to reproduce the experimental result within a factor of 2 (figure 8). The simple estimate is based on Eqn.5 with only a single activated jump, which is detrapping and is described by

$$D_{Detrap} = \frac{N}{6} \left(\frac{\omega^{Detrap} (L^{Detrap})^2}{\sum_{i=1}^N (-\ln(U_i))} \right) \quad (7)$$

where D_{Detrap} is the diffusion co-efficient due to trapping-detrapping at the internal porosity sites of graphite. A detrapping event from an internal surface leads to the hydrogen atom flying across the void in a random direction till it either adsorbs at another internal surface or gets out of the graphite. Therefore the jump size for a detrapping event is of the order of the void size in graphite ($L^{Detrap} = L^{void}$). The good match between the simple estimate and experiment indicates that the diffusion of hydrogen atoms in the graphite scales as the square of the void size.

4.3. Hydrogen atom transport in graphites with closed pores

Transport and retention in graphite with closed pores is of interest as part of optimizing the graphites to make them suitable as first wall materials in fusion devices. Closed pore graphites are created by increasing the graphitization temperature of doped graphite during the production process of graphite [22]. Closed pores can reduce the accessibility of internal surface areas within the graphite, thereby reducing the area available for hydrocarbon formation and hydrogen retention. This can have implications for chemical erosion and hydrogen isotope inventory in graphites. We study the effect of closed pores by artificially keeping the surface cells (cubes of size $5 \times 10^{-7}m$) occupied. This implies that there are no open voids leading out from a depth of $5 \times 10^{-7}m$ inside the graphite sample to the surface, though voids may exist as usual along all other directions. The hydrogen atoms are initialized around $6 \times 10^{-7}m$ with a spread of $1 \times 10^{-9}m$, and are allowed to diffuse in the sample kept at temperatures of 300 K, 600 K, 900 K, 1200 K and 1500 K. The simulation is repeated without closing the pores for comparison and the results are presented below.

The particle positions in the 3D porous structure at the end of 10^6 steps at 300 K, 900 K and 1500 K, for both, closed pores and open pores are shown in the \mathbf{Z} direction in figure 9. Filled circles represent atoms in granules and the empty circles represent atoms in voids. The graphite surface is situated at $\mathbf{Z} = 0$. It is seen that most of the diffusion broadening is due to surface diffusion of atoms in the voids. At 1500 K the

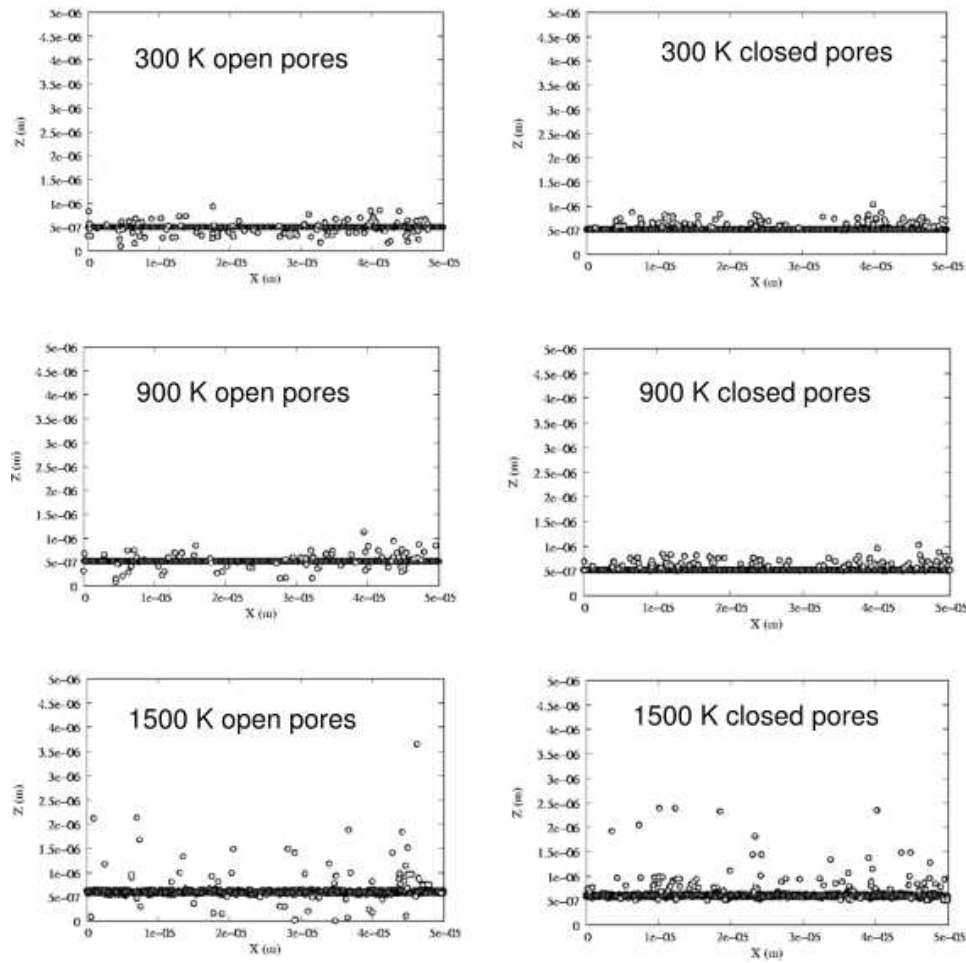


Figure 9. H atom positions at the end of 10^6 steps for different graphite temperatures for open and closed pore cases. The surface lies at $Z = 0$.

atoms in the granules too show some diffusion broadening in both cases. Note that there is no diffusion into closed pore region ($Z \leq 5 \times 10^{-7} m$) for the 900 K and 300K *closed pores* cases. In the 1500 K *closed pores* case there is some diffusion into the closed pores region as expected.

The above idealized example suggests that when closed pore graphites are used as plasma facing materials, the diffusion into the bulk of the graphite will be hindered and the hydrogen inventory within the graphite bulk in such cases will be reduced.

5. Summary and outlook

We have carried out multi-scale simulations of trace hydrogen atom transport in porous graphite and have demonstrated the effect of the internal structure of graphite on atomic hydrogen transport. Specifically we have shown that:

- Trace diffusion coefficients of atomic hydrogen in porous graphite vary as the square

of the void size of the graphite.

- Diffusion along internal surfaces dominates at temperatures < 1200 K. Above 1200 K the adsorption–desorption mechanism begins to dominate inspite of its larger migration energies. This is due to larger possible jump size after desorption, which depends on the void sizes.
- Diffusion coefficients have to be interpreted taking into account the disordered internal surfaces, not only in simulations, but also when reporting experimental results.
- Closed pore graphites can prevent diffusion along internal surfaces deep into the graphite bulk and will minimize the effective surface available for hydrocarbon formation and hydrogen retention.

Acknowledgments

M. Warriier acknowledges funding for the collaboration from the Max-Planck India Fellowship. R. Schneider acknowledges funding of the work by the Initiative and Networking Fund of the Helmholtz Association.

References

- [1] K. L. Wilson et. al. Trapping, detrapping and release of implanted hydrogen isotopes. *Atomic and plasma-material interaction data for fusion (supplement to the journal Nuclear Fusion)*, 1:31–50, (1991).
- [2] Wolfhard Möller. Hydrogen trapping and transport in carbon. *J. Nucl. Mater.*, 162-164:138–150, (1989).
- [3] A. A. Haasz, P. Franzen, J. W. Davis, S. Chiu, and C. S. Pitcher. Two-region model for hydrogen trapping in and release from graphite. *J. Appl. Phys.*, 77(1):66–86, (1995).
- [4] G. Federici and C.H. Wu. Modelling of plasma hydrogen isotope behavious in porous materials (graphites/carbon-carbon composites). *J. Nucl. Mater.*, 186:131–152, (1992).
- [5] A. Hassanein, B. Wiechers, and I. Konkashbaev. Tritium behaviour in eroded dust and debris of plasma-facing materials. *J. Nucl. Mater.*, 258-263:295–300, (1998).
- [6] M. Mayer, M. Balden, and R. Behrisch. Deuterium retention in carbides and doped graphites. *J. Nucl. Mater.*, 252:55–62, (1998).
- [7] R. A. Causey, M. I. Baskes, and K. L. Wilson. The retention of deuterium and tritium in poco axf-5q graphite. *J. Vac. Sci. Technol. A*, 4(3):1189–1192, (1986).
- [8] J. Küppers. The hydrogen surface chemistry of carbon as a plasma facing material. *Surface Science Reports*, 22:249–321, (1995).
- [9] M. Warriier, R. Schneider, E. Salonen, and K. Nordlund. Modeling of the diffusion of hydrogen in porous graphite. *Physica Scripta*, T108:85, (2004).
- [10] M. Warriier, R. Schneider, E. Salonen, and K. Nordlund. Multi-scale modelling of hydrogen isotope diffusion in graphite. *Contrib. Plasma Phys.*, 44(1-3):307–310, (2004).
- [11] M. Warriier, R. Schneider, E. Salonen, and K. Nordlund. Multi-scale modeling of hydrogen isotope transport in porous graphite. *Jnl. Nucl. Mater.*, 337-339:580–584, (2005).
- [12] K.A. Fichthorn and W.H. Weinberg. Theoretical foundations of dynamical monte carlo simulations. *J. Chem. Phys.*, 95(2):1090–1096, (1991).
- [13] A. B. Bortz, M. H. Kalos, and J. L. Lebowitz. A new algorithm for monte carlo simulation of ising spin systems. *J. Computational Physics*, 17:10, (1975).

- [14] P. E. Kloeden and E. Platen. Numerical solution of stochastic differential equations. *Springer series in Applications of Mathematics*, 23, (1999).
- [15] F. Graziani. Radiation transport in heterogeneous materials. *APS meeting : Conference on Computational Physics 2002*, August 25-28(San Diego), (2002).
- [16] M. V. Smoluchowski. *Z. physik. Chem.*, 92:192, (1917).
- [17] W. Eckstein. Computer simulations of ion–solid interactions. *Springer series in material science 10*, Springer-Verlag, (1991).
- [18] W. Eckstein. Calculated sputtering, reflection and range values. *Rep. IPP 9/132, Max-Planck-Institut für Plasmaphysik, Garching, Germany*, (2002).
- [19] K. Ashida, K. Ichimura, M. Matsuyama, and K. Watanabe. Thermal desorption of hydrogen, deuterium and tritium from pyrolytic graphite. *J. Nucl. Mater.*, 128 & 129:792, (1984).
- [20] P. Franzen and E. Vietzke. Atomic release of hydrogen from pure and boronized graphites. *J. Vac. Sci. Technol. A*, 12(3):820–825, (1994).
- [21] S. Havlin and D. Ben-Avraham. Diffusion in disordered media. *Adv. Phys.*, 51(1):187–292, (2002).
- [22] M. Balden, E. Oyarzabal, E. de Juan Pardo, K. Durocher, J. Roth, and C. García-Rosales. Deuterium retention by implantation in carbide–doped graphites. *Physica Scripta*, T103:38–42, (2003).